

# Simultaneous State and Parameter Estimation Method for a Conventional Ozonation System

Isaac Chairez<sup>1,†</sup>, Asif Chalanga<sup>2</sup>, Alex Poznyak<sup>3</sup>, Sarah Spurgeon<sup>2</sup> and Tatyana Poznyak<sup>4</sup>.

**Abstract**—This article presents a simultaneous state (via a nonlinear form of Luenberger observer) and parameter (using a proportional-integral least mean square form) estimator design method for a conventional ozonation system. The suggested state observer assumes that the only available output signal is the concentration of the ozone gas at the output of the reactor. The estimation of the reaction rate constants of ozonation in the presence of contaminants uses the suggested proportional-integral estimation method. The convergence proof of the developed state-parameter identification method was confirmed using a Lyapunov based stability analysis. This analysis characterizes the quality of estimation considering the presence of modeled uncertainties and external perturbations. The implementation of the super-twisting algorithm as a robust and exact differentiator allowed to perform the estimation of the reaction rate constants of the ozonation, the temporal evolution of the dissolved ozone and the evolution of contaminants concentrations. The simultaneous state and parameter estimator design method was implemented in real-time using phenol as a model contaminant. The numerically simulated and real-time implementations showed that the method provides accurate estimates of the contaminant concentration and the reaction rate coefficient in all the evaluated cases.

**Keywords:** Conventional ozonation; Super-twisting algorithm; Proportional-integral parametric identifier; Simultaneous state-parameter estimator.

## 1. INTRODUCTION

The ozonation of organic compounds is a mature technology to decompose toxic compounds from wastewaters, contaminated soil, or gas streams. Wastewater treatment by ozone has been applied in the industry with remarkable results [1], [2], [3]. Ozonation is the fastest chemical oxidation reaction performed in reactors where this gas must be dissolved in a liquid, solid, or another gas [4], [5]. The dissolved ozone can react with other organic and inorganic compounds yielding their complete decomposition or transformation into simpler and less toxic compounds [6].

Wastewater treatment by ozone can produce purified water streams that can be used in different human activities and industrial processes [7], [8]. This treatment uses technological equipment consisting of the ozone generator and sensor and the chemical reactor system [9], [10]. However, it is not easy to characterize the ozonation effectiveness because the evolution of the contaminants (in many cases) cannot be obtained online.

Moreover, the impossibility of measuring the contaminant concentrations limits the kinetic analysis of the ozonation reaction [11], [12]. The interactions between compounds through partial or complete oxidation in the treated waters also occur. These are extremely important for environmental engineering. The kinetic analysis of the chemical interactions may be used to achieve the optimal ozonation regime. The realization of ozonation in this optimal regime is needed to justify the applied wastewater treatment's effectiveness (chemical and economic).

Mathematical modeling of ozonation serves as an auxiliary tool to realize the kinetic analysis. The ozonation models are based on the material balance for the ozone mass transfer and the chemical reactions of contaminants with ozone. Usually, these models are represented by ordinary differential equations (ODEs) assuming a perfect stirring in the chemical reactor [13]. Otherwise, the application of models given by partial differential equations (PDEs) is required [14]. The states of such models include a) the ozone concentration in the head-space of the reactor (gaseous), b) the dissolved ozone in the liquid (water) phase, and c) the concentration of the chemical compounds reacting with ozone.

Notice that measuring all the components participating in the ozonation is unfeasible. The interaction of ozone and the contaminants themselves yields a sequence of series and parallel reactions forming several intermediates and final products. The successful analysis of the ozonation reaction and its control demands complete knowledge of all the states of the process. This need is the primary justification for the application of state observation (usually known as software sensors) and parameter estimation as an important combined solution for the study of chemical processes and corresponding effective controller design.

There are limited approaches dealing with the challenging problem of simultaneously estimating the states and parameters in chemical engineering. This problem is known as simultaneous state and parameters estimation of dynamic systems [15]. The current concurrent parameter and state estimation is now a mature theory. This study takes advantage of many previous results that have proposed the application of gradient descendant formulations with derivative and integral components. This technique has been successfully applied for bioreaction systems considering the limited knowledge of microbial growth rate and the state variation [16], [17], [18]. These previous approaches used well-settled mathematical abstractions of the systems under analysis. In particular, this study presents a modified version of this estimator for a class of mass balance and an integrated kinetic model of

<sup>1</sup> Tecnológico de Monterrey Campus Guadalajara, Jalisco, Mexico and UPIBI, Instituto Politécnico Nacional, Mexico City, Mexico. Tel. (+52) 55 57 29 60 00 Ext. 56351. E-mail: isaac.chairez@tec.mx, jchairezo@ipn.mx.

<sup>2</sup> Department of Electronic and Electrical Engineering, University College London, London WC1E 7JE, UK.

<sup>3</sup> Automatic Control Department, Centro de Investigación y Estudios Avanzados, Mexico City, Mexico.

<sup>4</sup> SEPI, Escuela Superior de Ingeniería Química e Industrias Extractivas, Instituto Politécnico Nacional, Mexico City, Mexico.

<sup>†</sup> The corresponding author.

ozonation for a class of batch reaction systems. The proposed formulation takes advantage of the admissible mathematical model of the ozonation system and derives a sequence from estimating both states and parameters.

An alternative solution uses the concept of Differential Neural Networks [19] may solve this problem even if the mathematical model is not entirely known. The state and parameter estimation procedure has a rather complex structure, including nonlinear matrix learning reinforcement laws. Moreover, the obtained non-parametric model has no direct physical interpretation. Here, a model generated and validated from the material balance and chemical kinetics is used, which brings a more precise physical interpretation to the estimated states and parameters.

This paper aims to suggest a method for the effective on-line simultaneous estimation of both the contaminant concentration and the corresponding reaction rate constants with ozone. The contaminant reconstruction is realized by a Luenberger-type observer implementation, and the parameter identification uses a Proportional-Integral (PI) version of the continuous Least Square Method (LSM).

Ozonation reaction systems present several complexities that have prevented their application on a large scale.

- There is poor information on the reaction conditions because the contaminant concentrations cannot be measured online, or sensors are prohibitively expensive for implementation.
- The measurable information corresponds to the ozone concentration at the reactor's input and output.
- There is no preliminary information about the exact reaction rate constants of the contaminants that may participate in the ozonation, but sometimes, feasible ranges of the constants are available.

This study contains the following main contributions:

- The design of a joint parameter-state estimation scheme for ozonation systems with uncertain reaction rate constants. The formal convergence analysis of the simultaneous estimation of the state and parameters can be obtained by applying the Lyapunov stability method.
- The development of a simultaneous state (via a nonlinear form of Luenberger observer) and parameters (using a proportional-integral least mean square form) estimation method.

This paper is organized as follows: Section II contains the description of the ozonation mathematical model for several contaminants. Section III establishes the problem statement for estimating the states and the reaction rate constants simultaneously. Section IV details the design of the estimators for either the states and the reaction rates. Section V provides some numerical results using the ozonation reaction model with one (representing the phenol) and two contaminants (considering phenol and 4-chlorophenol). Section VI describes the evaluation of the proposed estimator using real experimental data considering phenol as the contaminant. The final section closes the article with some concluding remarks.

## 2. MODEL DESCRIPTION

### 2.1. Ozonation reaction system

The ozonation reaction is usually performed in a semi-batch reactor: ozone is continuously injected into the reactor with a constant flow and concentration. The contaminant to be decomposed is dissolved in the liquid phase (wastewater) in the reactor. The unused ozone concentration in the reactor output was measured by the online analyzer. Figure 1 describes the ozonation's system, which is formed by the oxygen tank, the electrical generator, the glass reactor, the ozone detector, and an electronic device used to collect the ozone concentration at the reactor head-space.

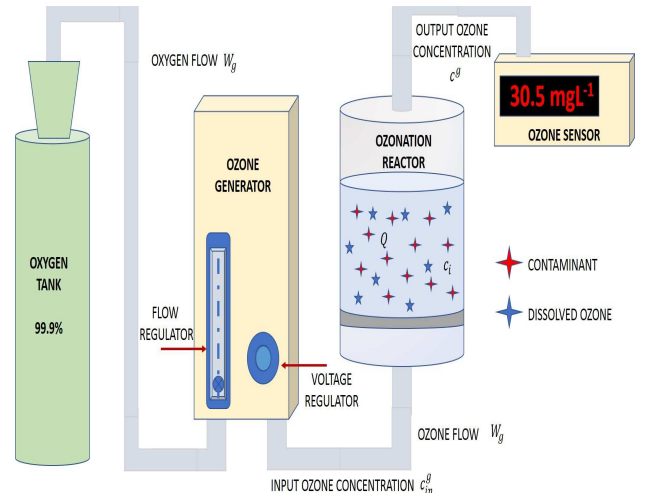


Fig. 1. Ozonation system including the oxygen tank, the ozone generator, the ozonation reactor and the ozone monitoring device.

### 2.2. Material balance in integral form

The following set of equations corresponds to the mathematical model of ozonation when the contaminants  $c_i$  are included. First, the general model for the ozone concentration in the gaseous phase  $c^g$  in integral form corresponds to:

$$\left. \begin{aligned} \int_0^t W_g(\tau) c_{in}^g(\tau) d\tau &= \int_0^t W_g(\tau) c^g(\tau) d\tau + \\ &V_g c^g(t) + Q(t) \\ c^g(0) &= c_0^g \end{aligned} \right\} \quad (1)$$

where  $c_{in}^g$  [ $mole \cdot L^{-1}$ ] is the ozone concentration at the reactor input,  $c^g$  are the current ozone concentrations in the gaseous phase [ $mole \cdot L^{-1}$ ],  $W_g$  is the gas flow-rate [ $L \cdot s^{-1}$ ],  $V_g$  is the volume of the gas phase [ $L$ ],  $Q$  is the current ozone amount in liquid phase [ $mole$ ].

*Remark 1:* The equation (1) can be used as it considers the direct relationship between the ozone concentration measured at the reactor's output and the one dissolved in the liquid phase. Your suggestion could be helpful to construct the close form of the ozone estimation in  $Q$ , but this could provoke that the output information will converge to the estimated one  $\hat{Q}$  which could eliminate the identifiability property of the suggested system.

The dynamics of the dissolved ozone  $Q$  admits

$$\frac{d}{dt}Q(t) = k_{sat}(Q_{max} - Q(t)) - Q(t) \sum_{i=1}^N k_i c_i(t) \quad (2)$$

The first term in (2) defines the mass transfer of ozone through the diffusion filter (gaseous to liquid phases). There are experimental pieces of evidence that such a process is governed by first-order kinetics with respect to the gradient of the current ozone and maximal ( $Q_{max}$  [mole]) ozone concentrations. The maximum value can be estimated using Henry's law (assuming that the ozone reactor runs under controlled temperature conditions). The ozone mass transfer is regulated with the transfer constant  $k_{sat}$  [ $s^{-1}$ ]. Several studies proved that dissolved ozone dynamics are proportional to the difference between the maximum dissolved and current ones. Among the most celebrated, the studies presented in [20], [21] justified such relationship. These cites have been included in the reviewed manuscript.

The ozone consumption due to the kinetic reaction with the contaminants  $c_i$  ([mole  $\cdot$  L $^{-1}$ ]) is characterized in the second term of (2) which establishes the second-order reaction between molecular ozone and the contaminants. The reaction rate between ozone and each contaminant is characterized by  $k_i$ . The high reactivity of ozone with other organics (taking into consideration the oxidation number of this compound) allows considering the bimolecular model is considered valid. This fact has been demonstrated when ozone reacts with organics, including phenols and their derivatives. Experimental evaluations have validated such a claim in different seminal chemical studies such as the ones presented in [22], [23], [24], [25].

### 2.3. Stoichiometric reaction between ozone and contaminants

The kinetic reaction between ozone and the contaminant is described by a bimolecular kinetic equation:

$$\frac{d}{dt}c_i(t) = -k_i \frac{Q(t)}{V_{liq}} c_i(t) \quad i = \overline{1, N} \quad (3)$$

where  $c_i$  [mole  $\cdot$  L $^{-1}$ ] is the concentration of the  $i$ -th contaminant in the reactor,  $k_i$  [L  $\cdot$  mole $^{-1}$   $\cdot$  s $^{-1}$ ] defines the reaction rate constant between ozone and the  $i$ -th contaminant and  $V_{liq}$  [L] is the liquid volume. The bi-molecular reaction model in (3) is justified because the relative selectivity of ozone reacting with different organic compounds.

### 2.4. State representation of the ozonation model

The model presented in equations (1-3) can be represented in a more abstract form. This structure uses the state variable theory. In an extended format, the ozonation reaction system satisfies:

$$\left. \begin{aligned} \frac{d}{dt}c^g(t) &= V_g^{-1}W_g(c_{in}^g - c^g(t)) - \\ &V_g^{-1} \left[ k_{sat}(Q_{max} - Q(t)) - Q(t) \sum_{i=1}^N k_i c_i(t) \right] \\ \frac{d}{dt}Q(t) &= k_{sat}(Q_{max} - Q(t)) - \\ &Q(t) \sum_{i=1}^N k_i c_i(t) \\ \frac{d}{dt}c_i(t) &= -k_i \frac{Q(t)}{V_{liq}} c_i(t) \quad i = \overline{1, N} \\ y(t) &= c^g(t) \end{aligned} \right\} \quad (4)$$

The model (4) is obtained from the direct differentiation of (1), the dissolved ozone variation in (2) as well as the contaminants dynamics presented in (3).

*Remark 2:* Note that this model has an equilibrium point at the origin. At this point, all the concentrations are zero. In this case, the asymptotic solution of the state or parameter estimation problem is not useful. It is necessary to realize **estimation during the transient period**.

The saturation constant of dissolved ozone can be estimated by the solution of the following nonlinear regression equation [26]

$$k_{sat} = \frac{W_g(c_{in}^g - c^g(t^*))}{Q_{max}} e^{k_{sat}t^*}$$

where  $t^*$  is the time when the ozone gas concentration is minimum (See figure 2). The maximum value of dissolved ozone  $Q_{max}$  can be calculated by the following equation based on Henry's law

$$Q_{max} = HV_{liq}c_{in}^g \quad (5)$$

where  $H$  is the so-called *Henry's constant*.

## 3. PROBLEM FORMULATION

*Problem 1:* Based on the output ozone concentration data  $c^g$ , estimate the variation of the contaminants' concentrations  $c_i$  as well as the corresponding reaction rate constants  $k_i$ . The problem must be solved under the assumption that no initial conditions of  $c_i$  are available.

Notice that the only online available data is  $c^g$  which can be measured by the corresponding ozone analyzer (see Figure 1). The information collected from this sensor is noisy (see the ozonogram in Figure 2):

The information collected in the ozone contraction at the reactor's output can be used considering that it indirectly shows the ozone consumption during the ozonation. Intending to show this fact, Figure 3 depicts the evolution of ozone concentration when two contaminants are ozonated (phenol and chlorophenol) together. Notice the higher ozone consumption compared to the one considered in Figure 2.

The experimental conditions for getting the ozone concentration reported in Figure 2 are the following: Input ozone concentration was 37.0 g  $\cdot$  L $^{-1}$ , ozone gas flow of 0.5L  $\cdot$  s $^{-1}$ , a static gas diffuser with diameter pore 0.2  $\mu$ m and a distilled water volume of 0.7 L in one liter glass reactor. These experimental conditions were selected to remove the effect of

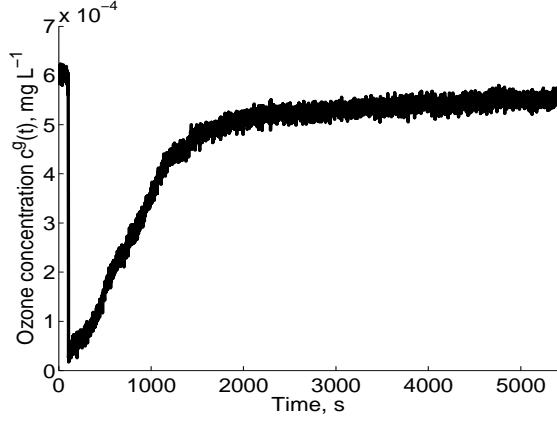


Fig. 2. Ozone concentration measured at the reactor output during the ozonation of a single contaminant.

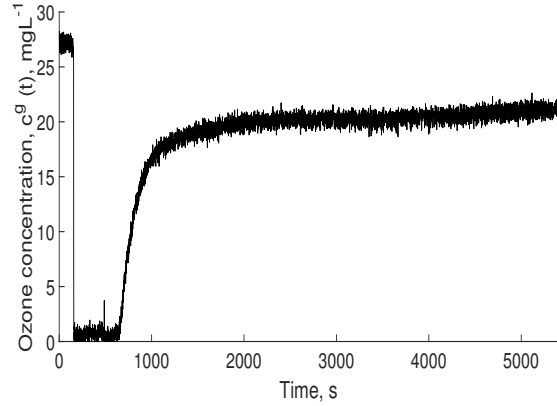


Fig. 3. Ozone concentration measured at the reactor output during the ozonation of two contaminants.

contaminants' reaction with ozone. Therefore, the estimation of  $k_{sat}$  can be gotten precisely.

The estimation of all contaminants' concentrations can be used to define the time instant when the ozonation finishes and the treated wastewater can be considered purified. Indeed, if the estimated concentrations are obtained online, they can be compared to the values proposed in the local environmental regulations. Therefore, the ozonation can be stopped if all the contaminants' concentrations are below their corresponding permissible values.

#### 4. STATE AND PARAMETER ESTIMATOR AS A SOFTWARE SENSOR

This section describes the method designed to simultaneously estimate the states and parameters of the ozonation system. The first part of this algorithm assesses the dissolved ozone in the liquid phase. The second part introduces a proportional-integral form to reconstruct the parameters in the reaction equation of the contaminant.

##### 4.1. Estimation of dissolved ozone

The estimate  $\hat{Q}(t)$  of dissolved ozone  $Q(t)$  can be obtained by the direct use of the material balance equation in integral

form (1):

$$\hat{Q}(t) = \hat{Q}(0) + \int_0^t W_g(\tau) (c^g(\tau) - c_{in}^g(\tau)) d\tau + V_g (c^g(t) - c^g(0)) \quad (6)$$

Notice that for equation (6),  $\hat{Q}(0) = 0$  can be fixed under the selected experimental conditions.

##### 4.2. Estimate of reaction rate constants and contaminant concentrations

The method to estimate the reaction constant is realized according to the following procedure:

$$\left. \begin{aligned} \frac{d}{dt} \bar{k}_i(t) &= -\alpha_i(t) J_i(t) - \delta_{P_i} [\hat{k}_i(t) - \dot{k}_i] - \delta_{I_i} \int_{\tau=0}^t [\hat{k}_i(\tau) - \dot{k}_i] d\tau \\ \hat{k}_i(t) &= \Pr \{ \bar{k}_i(t) \}^{k_i^+}, \quad 0 < \dot{k}_i < k_i^+ < +\infty \\ \frac{d}{dt} J_i(t) &= (t + \varepsilon)^{-1} (g_i(t) - J_i(t)), \quad \varepsilon > 0 \\ J_i(0) &= 0, \quad \delta > 0, \quad \alpha_i(t) > 0, \quad \int_0^\infty \alpha_i(t) dt = \infty \\ g_i(t) &= -[\mathbf{P}(t) - \hat{\mathbf{P}}(t)] [1 - \hat{k}_i(t) \varphi(t)] \\ \varphi(t) &= V_{liq}^{-1} \int_0^t \hat{Q}(s) ds \end{aligned} \right\} \quad (7)$$

where  $\dot{k}_i$  is a nominal value reported in literature.

The structure in (7) is a class of PI observer aided with projection. This projection considers the necessity of restricting the estimated reaction rate  $k_i$  as a positive value and imposing a max bound that is used later on in the proof of the convergence to the actual values of the reaction rate constant. The proportional part of the observer obeys the classical gradient descendant algorithm, with the additional correction of the integral section. Such a part helps correct the estimation if the associated functional  $J_i(t)$  becomes insensitive to the estimated gain variation.

The nominal values of  $k_i$  were taken from previous studies dealing with the characterization of the ozonation reaction for similar contaminants. Notice that such values give starting points to the method (7) which helps accelerate the estimation of the reaction rate constants.

The functional  $J_i(t)$  operates as the correcting element of the reaction rate constant estimation endorsed with the method in (7). The function  $g_i(t)$  plays the role of the regression term, which takes into account the estimation error for all constants. This design provides a class of simultaneous estimation for all the rate constants in the ozonation system with several contaminants. The values of  $\delta_{P_i}$ ,  $\delta_{I_i}$ , and  $l_i$  are obtained with a recursive method.

The estimate  $\hat{\mathbf{P}}$  of  $\mathbf{P}$  satisfies

$$\hat{\mathbf{P}}(t) = \sum_{i=1}^N \hat{\mathbf{P}}_i(t), \quad \hat{\mathbf{P}}_i(t) = -\hat{k}_i \hat{Q}(t) \hat{c}_i(t) \quad (8)$$

The projection operator in the method presented in (7) satisfies:

$$\Pr \{ \bar{\xi}_i \}_{0}^{\xi_i^+} := \begin{cases} \xi_i^+ & \text{if } \bar{\xi}_i > \xi_i^+ \\ \xi_i & \text{if } \bar{\xi}_i \in [0, \xi_i^+] \\ 0 & \text{if } \bar{\xi}_i < 0 \end{cases}$$

The value of  $\mathbf{P}(t) := -\sum_{i=1}^N k_i Q(t) c_i(t)$  can be calculated from

$$\mathbf{P}(t) = k_{sat}(Q_{\max} - \hat{Q}(t)) - \frac{d}{dt} \hat{Q}(t) \quad (9)$$

The realization of  $\mathbf{P}(t)$  requires the estimation of  $\frac{d}{dt} \hat{Q}(t)$  which can be obtained by the Super-Twisting algorithm (STA) [27], [28]:

$$\left. \begin{aligned} \frac{d \tilde{Q}(t)}{dt} &= k_{sat}(Q_{\max} - \hat{Q}(t)) + z(t) + \\ &\quad \gamma_1 \sqrt{|\Delta(t)|} \text{sign}(\Delta(t)) \\ \frac{dz(t)}{dt} &= \gamma_2 \text{sign}(\Delta(t)), \quad \Delta := \tilde{Q} - \hat{Q} \end{aligned} \right\} \quad (10)$$

The constants in the STA  $\gamma_1$  and  $\gamma_2$  must satisfy [27]:

$$\gamma_2 > \rho \\ \gamma_1 > 1.41 \sqrt{\gamma_2 + \rho}$$

This study uses the simplest form of the STA with constant gains. In recent results [29], [30], more precise estimation of the converging time has been issued as well as the way of analyzing the effect of time and state-dependent perturbations.

Based on the character of the ozonation variables, it may be concluded that

$$\rho > Q_{\max} \left[ \left( k_{sat} + \sum_{i=1}^N k_i c_i(0) \right)^2 + \sum_{i=1}^N k_i^2 \frac{Q_{\max}}{V_{liq}} c_i(0) \right]$$

The value of  $\mathbf{P}(t)$  can be estimated, namely  $\hat{\mathbf{P}}(t)$ , as

$$\hat{\mathbf{P}}(t) \simeq k_{sat}(Q_{\max} - \hat{Q}(t)) - \frac{d \tilde{Q}(t)}{dt}$$

The estimates of  $\hat{c}_i(t)$  in (8) can be obtained as follows:

$$\frac{d}{dt} \hat{c}_i(t) = \frac{\hat{\mathbf{P}}_i(t)}{V_{liq}} + l_i \left[ \mathbf{P}(t) - \hat{\mathbf{P}}(t) \right] \\ \hat{c}_i(t) = \Pr \{ \bar{c}_i(t) \}_{0}^{c_i^+}$$

where  $l_i$  is a positive scalar, which should be adjusted to enforce the convergence of  $\hat{c}_i$  to  $c_i$ ,  $i = 1, \dots, n$ . The upper-value used in the projection operator  $c_i^+$  can be fixed as  $c_i^+ = c_i(0)$ , which is known in advance.

The convergence analysis of the simultaneous estimation of the state and parameters can be obtained by applying the Lyapunov stability method (see a similar approach in [31]). This analysis is presented in the following section.

## 5. CONTRIBUTION OF THIS STUDY

This section describes the main contribution of this study that corresponds to the novel identifier based on the proportional-integral form using the estimates produced by the STA.

Lets introduce the auxiliary vector  $z^\top = [z_1^\top \cdots z_N^\top]$ ,  $z \in \mathbb{R}^{4N}$ ,  $z_i \in \mathbb{R}^4$ ,  $z_i^\top = [\Delta_{k_i} \ \hat{l}_i \ J_i \ \Delta c_i]$ . The dynamics of  $z$  is given by

$$\frac{d}{dt} z(t) = \Lambda^0 z(t) + (\Lambda(t) - \Lambda^0) z(t) + \Gamma(t) \quad (11)$$

where  $\Lambda^0$  is a Hurwitz matrix of appropriate dimensions ( $\Lambda^0 \in \mathbb{R}^{4N \times 4N}$ ) and

$$\Lambda(t) = \begin{bmatrix} \Lambda_{1,1}(t) & \Lambda_{1,2}(t) & \cdots & \Lambda_{1,N}(t) \\ \Lambda_{2,1}(t) & \Lambda_{2,2}(t) & \cdots & \Lambda_{2,N}(t) \\ \vdots & \vdots & \ddots & \vdots \\ \Lambda_{N,1}(t) & \Lambda_{N,2}(t) & \cdots & \Lambda_{N,N}(t) \end{bmatrix}, \\ \Gamma(t) = \begin{bmatrix} \Gamma_1(t) \\ \Gamma_2(t) \\ \vdots \\ \Gamma_N(t) \end{bmatrix}$$

The components of  $\Lambda(t)$  and  $\Gamma(t)$  are

$$\Lambda_{i,i}(t) = \begin{bmatrix} -\delta_{P_i} & -\delta_{I_i} & -\alpha_i(t) & 0 \\ 1 & 0 & 0 & 0 \\ -\hat{c}_i(t) Q(t) & 0 & -a(t) & -\hat{k}_i Q(t) \\ \hat{c}_i(t) \frac{Q(t)}{V_{liq}} & 0 & 0 & -k_i \frac{Q(t)}{V_{liq}} \end{bmatrix}$$

$$\Lambda_{i,j}(t) = Q(t) \begin{bmatrix} 0 & 0 & 0 & 0 \\ 0 & 0 & 0 & 0 \\ -\hat{c}_j(t) & 0 & 0 & -\hat{k}_j \\ 0 & 0 & 0 & 0 \end{bmatrix}$$

$$\Gamma_i(t) = \begin{bmatrix} 0 \\ 0 \\ -\sum_{i=1}^N \Delta \hat{k}_i c_i(t) Q(t) \\ 0 \end{bmatrix}$$

where  $\Delta \hat{k}_i = \hat{k}_i - \check{k}_i$ . Notice that

$$\Lambda_{i,i}^0 = \begin{bmatrix} -\delta_{P_i} & -\delta_{I_i} & \alpha_i^- & 0 \\ 1 & 0 & 0 & 0 \\ 0 & 0 & a^- & 0 \\ 0 & 0 & 0 & k_i \frac{Q_{\max}}{V_{liq}} \end{bmatrix}, \alpha_i^- > 0, a^- < 0 \\ \Lambda_{i,j}^0 = 0_{4 \times 4}$$

The structure of  $\Lambda(t)$  justifies the following assumption:

**Assumption 1:** There exists a positive scalar  $q \in \mathbb{R}^+$  such that the following upper bound is valid

$$\| \Lambda(t) - \Lambda^0 \|^2 \leq q$$

with  $\Lambda^0$  a Hurwitz matrix.

Notice that the term  $\|\Gamma(t)\|_{\Pi}^2$  is absolutely bounded with respect to time, that is there is a positive scalar  $\beta \in \mathbb{R}^+$  such that

$$\sup_{t \geq 0} \|\Gamma(t)\|_{\Pi}^2 \leq \beta \quad (12)$$

with  $\beta = \lambda_{\max} \{\Pi\} N \cdot \Delta k^+ \cdot \Upsilon(0) \cdot Q_{\max}^2$ .

*Remark 3:* The projection operator  $\hat{k}_i(t) = \Pr \{ \bar{k}_i(t) \}_0^{k_i^+}$  justifies the existence of the upper bound  $\beta$ . Complementary, notice that the gain method (7) is input to state stable if it is taking into account that in the considered process, the second time-derivative of  $\hat{k}_i$  is bounded.

The following Lemma introduces the sufficient conditions to ensure that the origin is a practically stable equilibrium point of (11).

*Lemma 1:* If there exists a positive scalar  $\alpha$  and a positive definite  $P \in \mathbb{R}^{4N \times 4N}$  such that the following algebraic Riccati equation

$$\begin{bmatrix} P\Lambda_{\alpha}^0 + \Lambda_{\alpha}^{0\top}P + \dot{P} + \pi q I_{4N \times 4N} = 0 \\ \dot{P} & P \\ P & \pi I_{4N \times 4N} \end{bmatrix} > 0, \quad \dot{P} > 0, \quad \dot{P} \in \mathbb{R}^{4N \times 4N} \quad (13)$$

$$\Lambda_{\alpha}^0 = \Lambda^0 + \frac{1}{2}(1 + \alpha) I_{4N}$$

has a solution being positive definite,  $\pi$  a positive scalar and  $I_{4N}$  an identity matrix with dimensions  $(4N \times 4N)$ , then

$$\limsup_{t \rightarrow \infty} \|z(t)\| \leq \sqrt{\frac{\beta}{\alpha \cdot \lambda_{\min} \{P\}}} \quad (14)$$

*Remark 4:* Notice that (14) implies that the origin is a practical equilibrium point for (11). This means that the suggested estimation method for  $k_i$  can recover the actual value of the reaction rate constants for the ozonation process with a certain degree of confidence defined by the presence of uncertainties in the modeling characterized by  $\Delta_i k^+$ .

*Remark 5:* The solution of (13) can be obtained by the application of a numerical algorithm (Interior Point Method) using software such as Yalmip and Sedumi, which can be executed in Matlab.

## 6. SIMULATION RESULTS BASED ON THE MATHEMATICAL MODEL

This section describes the application of the simultaneous state and parameters estimator for the ozonation model, including one and two contaminants, as well as their application using real experimental data of one contaminant.

### 6.1. One contaminant case

The model presented in (4) with a single contaminant was considered to test the estimation method proposed here. The set of parameters used to evaluate the numerical simulation was:  $V_g = 0.2L$ ,  $V_{liq} = 0.7L$ ,  $k_{sat} = 0.5$ ,  $W_g = 0.5L \cdot \text{min}^{-1}$ ,  $Q_{\max} = 1.05 \cdot 10^{-5} \text{mole}$ ,  $k_1 = 9500.0L \cdot \text{mole}^{-1} \text{s}^{-1}$ ,  $c_{in}^g = 6.25 \cdot 10^{-4} \text{mole} \cdot L^{-1}$ ,  $c^g(0) = 0.0 \text{mole} \cdot L^{-1}$ ,  $Q(0) = 0.0 \text{mole}$ ,  $c_1(0) = 1.56 \cdot 10^{-4} \text{mole} \cdot L^{-1}$ . The numerical simulation were undertaken in Matlab/Simulink using integration method ODE 1 with the integration time step set at 0.0001 s.

Figures 4-7 depict the evolution of  $\tilde{Q}$ ,  $\hat{P}$ ,  $\hat{k}_1$ ,  $\hat{c}_1$  and their comparisons with respect to the actual values of the same variables. The actual values were obtained from the model (4). This comparison defined the quality of the estimates generated by the method developed in this study.

Figure 4 shows the variation of the estimated dissolved ozone  $\hat{Q}(t)$  (Dotted line) and its comparison with the simulated variation of  $Q(t)$  (Solid line). The horizontal dashed line represents the maximum ozone ( $Q_{\max}$ ) that can be dissolved in the liquid phase.

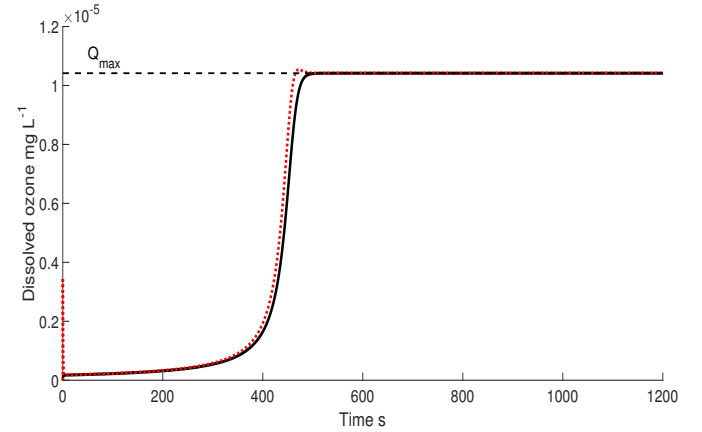


Fig. 4. The comparison of the modeled dissolved ozone (solid line) and the estimated by the method proposed in this study (dotted line). The  $Q_{\max}$  value appears as dashed line for reference.

The estimate of  $P(t)$  was obtained with the application of the STA. This differentiation algorithm was simulated with the parameters  $\gamma_1 = 0.65$ ,  $\gamma_2 = 1.35$ . The auxiliary estimate  $\hat{P}(t)$  tracks the actual value of  $P(t)$  after 5.0 seconds. The estimation was theoretically solved in finite time, as the STA method confirms (Figure 5).

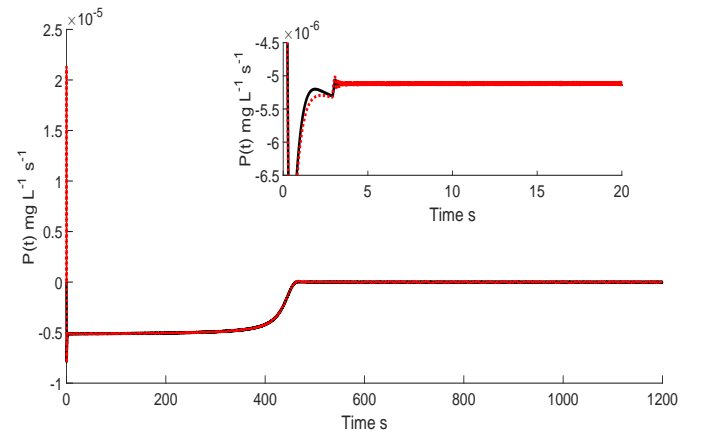


Fig. 5. The comparison of the modeled contaminant decomposition rate (solid line) and the estimated by the method proposed in this study (dotted line) based on the online reconstruction by the STA implemented as differentiator. The closer view demonstrates the first 20 seconds of simulation to highlight the faster estimation of  $P(t)$ .

Based on finite-time recovery of  $P(t)$ , estimation of the contaminant concentration was attained after 7.0 seconds. However, the linear nature of the parametric estimation method

introduces an asymptotic convergence of the contaminant estimation. Figure 6 demonstrates the comparison of the actual contaminant variation and its estimate. Notice that both trajectories decrease at the same rate.

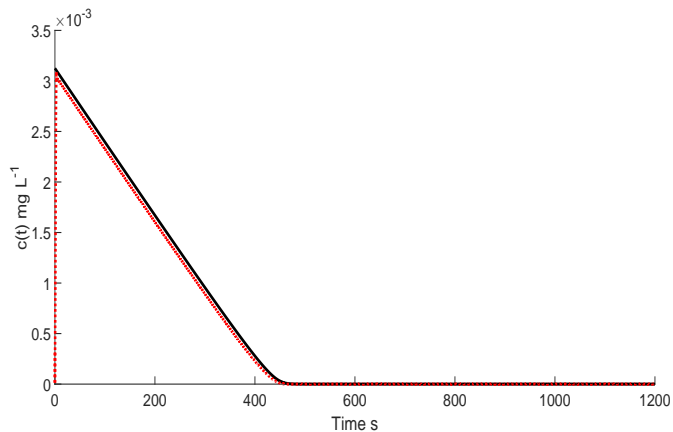


Fig. 6. The comparison of the modeled contaminant concentration  $c_1(t)$  (solid line) and the estimated by the method  $\hat{c}_1(t)$  proposed in this study (dotted line).

The parametric identification method proposed in (7) estimates the reaction rate constant  $k_1$  after 100 seconds. This estimation process asymptotically recovered the true value of the reaction rate constant of ozone with the proposed contaminant (Figure 7).

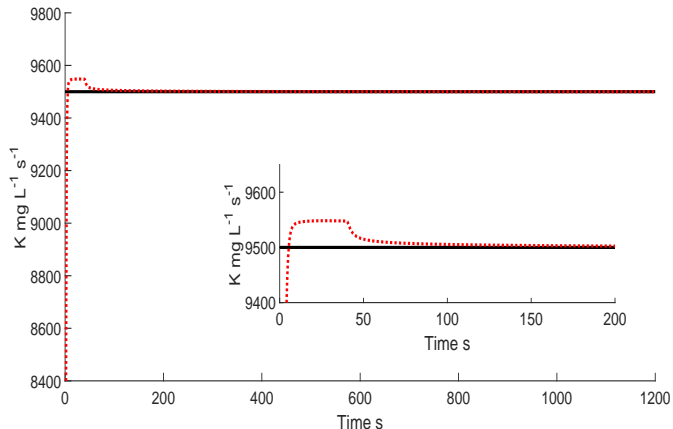


Fig. 7. The comparison of the modeled contaminant reaction rate constant  $k_1(t)$  (solid line) and the parameter estimated by the method  $\hat{k}_1(t)$  proposed in this study (dotted line).

## 6.2. Two contaminants case

The ozonation system with two contaminants was also considered in the evaluation process. This part of the study assumed that these two contaminants were not reacting among them. Also, the variation of the ozonation products was not considered. The considered parameters in the model come from previous studies reported in the literature. In particular, the reaction rate constants correspond to phenol and 4-chlorophenol.

The initial conditions for the model (4) were:

$$Q(0) = 0.0 \text{ mole}$$

$$c_1(0) = 1.56 \cdot 10^{-4} \text{ mole} \cdot \text{L}^{-1}$$

$$c_2(0) = 1.11 \cdot 10^{-4} \text{ mole} \cdot \text{L}^{-1}$$

The model (4) was simulated with the following parameters:

$$V_g = 0.2 \text{ L}, V_{liq} = 0.7 \text{ L}, k_{sat} = 0.5,$$

$$W_g = 0.5 \text{ L} \cdot \text{min}^{-1}$$

$$Q_{\max} = 1.05 \cdot 10^{-5} \text{ mole},$$

$$k_1 = 9500.0 \text{ L} \cdot \text{mole}^{-1} \text{ s}^{-1}$$

$$k_2 = 28000.0 \text{ L} \cdot \text{mole}^{-1} \text{ s}^{-1}$$

$$c_{in}^g = 6.25 \cdot 10^{-4} \text{ mole} \cdot \text{L}^{-1}$$

$$c^g(0) = 0.0 \text{ mole} \cdot \text{L}^{-1}$$

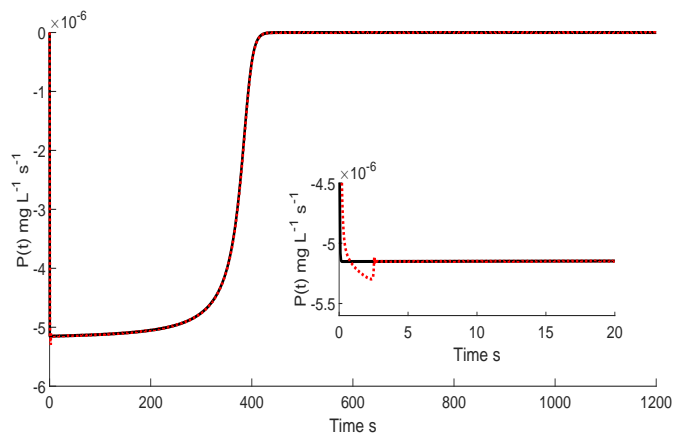


Fig. 8. The comparison of the modeled contaminants (two compounds case) decomposition rate (solid line) and the estimated by the method proposed in this study (dotted line) based on the on-line reconstruction by the STA implemented as differentiator. The closer view demonstrates the first 20 seconds of simulation to highlight the faster estimation of  $P(t)$ .

The estimate of  $P(t)$  in the case of ozonation of two contaminants was obtained by applying the STA. The used differentiation algorithm was simulated with the parameters  $\gamma_1 = 0.95$ ,  $\gamma_2 = 1.35$ . The auxiliary estimate  $\hat{P}(t)$  tracks the actual value of  $P(t)$  after 2.5 seconds which is half the time compared to the one contaminant case. The estimate was theoretically solved in finite time, as the STA method confirms (Figure 5).

The finite-time recovery of  $P(t)$  realizes the estimate of the first contaminant concentration, which was obtained after 3.0 seconds. The parametric estimation method produces asymptotic convergence of the contaminant estimate, but after 370 s, the difference between the actual contaminant concentration and its calculation is imperceptible.

Figure 9 demonstrates the comparison of the actual contaminant variation and its estimate. Notice that both trajectories decrease at the same rate.

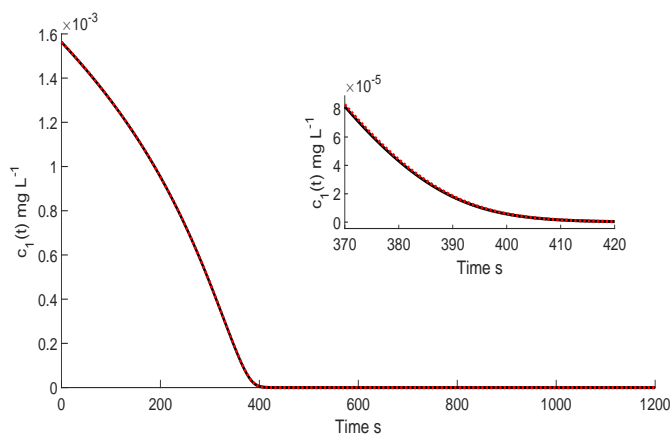


Fig. 9. The comparison of the first modeled measured contaminant concentration  $c_1(t)$  (solid line) and the estimated by the method  $\hat{c}_1(t)$  proposed in this study (dotted line) for the ozonation of two different contaminants.

Figure 10 demonstrates the comparison of the actual contaminant variation and its estimate for the second estimate. Notice that both trajectories decreases at the same rate.

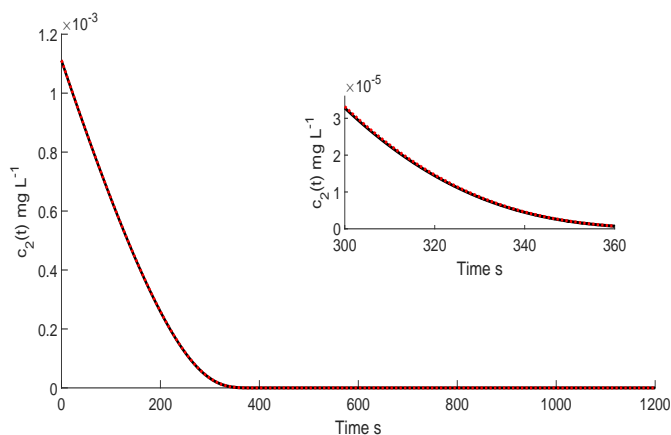


Fig. 10. The comparison of the second modeled contaminant concentration  $c_2(t)$  (solid line) and the estimated by the algorithm  $\hat{c}_2(t)$  proposed in this study (dotted line) for the ozonation of two different contaminants.

The parametric identification method proposed in (7) estimates the reaction rate constant  $k_1$  after 50 seconds and  $k_2$  after 25 seconds. This estimation asymptotically recovered the true value of the reaction rate constant of ozone with the proposed contaminant (Figure 11). The identification of the second constant was faster (25 seconds) for the second contaminant (Figure 12). Notice that this identification time difference is relevant because the second contaminant decomposes faster. The estimates of the reaction rate constants do not oscillate much over their actual value. This behavior appears because of the application of the projection method for both the gains and the estimated concentrations.

## 7. ESTIMATION BASED ON EXPERIMENTAL DATA

### 7.1. Chemical reagents

The studied organic pollutant was phenol ( $Ph$ ). This chemical was purchased from Aldrich Co of analytic grade.

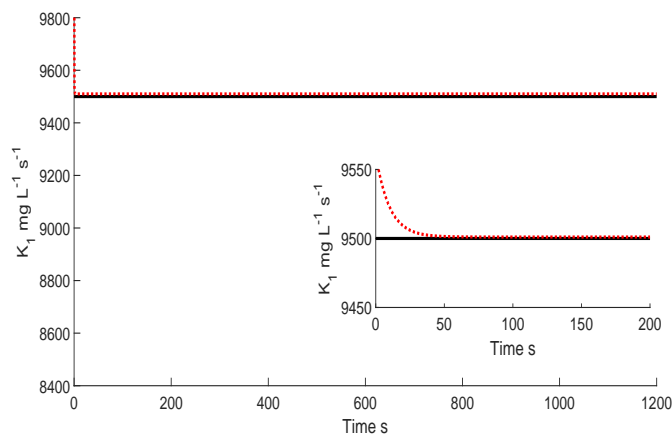


Fig. 11. The comparison of first modeled contaminant reaction rate constant  $k_1(t)$  (solid line) and the parameter estimated by the method  $\hat{k}_1(t)$  proposed in this study (dotted line) in the case of ozonation of two different contaminants.

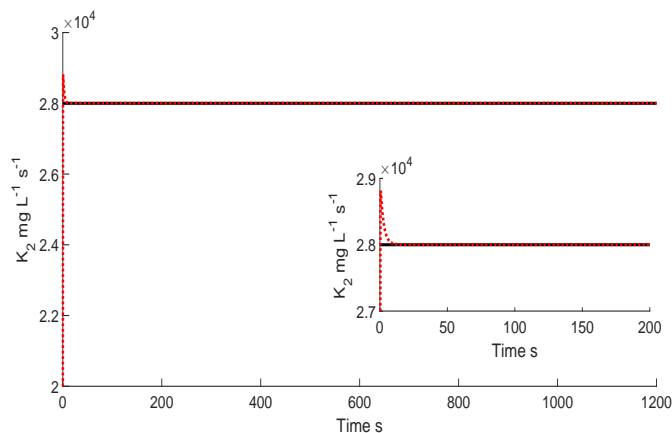


Fig. 12. The comparison of second modeled contaminant reaction rate constant  $k_2(t)$  (solid line) and the parameter estimated by the method  $\hat{k}_2(t)$  proposed in this study (dotted line) in the case of ozonation of two different contaminants.

### 7.2. Experimental conditions of ozonation

The ozonation of phenol was conducted with synthetic solutions in distilled water at the initial concentration of  $200 \text{ mg} \cdot \text{L}^{-1}$ . The reactor was of semi-batch type ( $0.5 \text{ L}$ ).

The initial ozone concentration was  $23 \text{ mg} \cdot \text{L}^{-1}$ . The ozone-oxygen mixture flow was  $0.5 \text{ L} \cdot \text{min}^{-1}$ . All experiments were carried out at  $20^\circ\text{C}$  with agitation by bubbling an ozone-oxygen mixture and by a magnetic agitation (operated at 120 rpm). All ozonation experiments were conducted using constant  $pH = 7$ . The  $pH$  variation was achieved with sulfuric acid and sodium hydroxide ( $0.1 \text{ N}$ ). All experiments' aliquots of  $3.0 \text{ mL}$  reaction solution were withdrawn at desired time intervals from the reactor for sequential analyses.

Ozone was generated from dry oxygen by the ozone generator (corona discharge type) HTU500G (“AZCO” Industries Limited – Canada). An Ozone Analyzer BMT 963 (BMT Messtechnik, Berlin) provided the ozone detection in the gas phase in the reactor outlet for the ozone monitoring to control the ozonation degree, the ozone consumption and the ozone decomposition.

### 7.3. Analytic methods

Identification of the phenol concentration has been achieved by high performance liquid chromatography (HPLC), by the liquid chromatography (Perkin Elmer) equipped with UV-Vis detector series 200 (190 – 460 nm).

A reverse-phase column was of C-18 (Nova Pack C-18, Waters), 300 mm in length and 3.9 mm in diameter. The mobile phase was combined as water–acetonitrile–phosphoric acid 50 : 50 : 0.1 for phenols.

### 7.4. Results

Figure 13 shows the variation of the estimated dissolved ozone  $\hat{Q}(t)$  (Solid line) and its comparison with the maximum value of  $Q(t)$  (dashed line), that is  $Q_{max}$ , when the method proposed in (6) was implemented using the experimental online ozone concentration. The maximum dissolved ozone ( $Q_{max}$ ) mass was estimated by implementing Henry's law. This calculus method has been confirmed in previous studies such as [19].

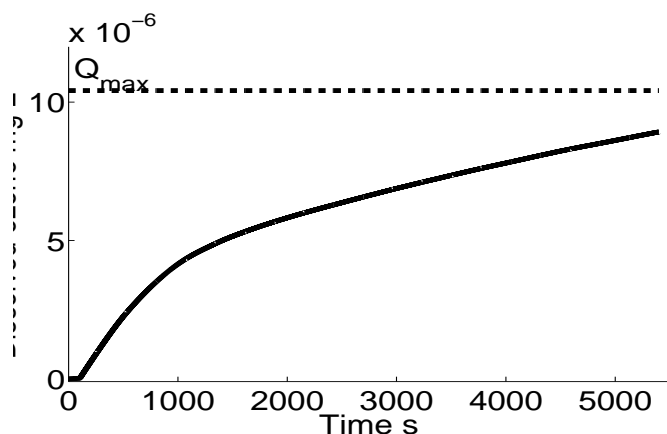


Fig. 13. The comparison of estimated dissolved ozone (solid line) and the  $Q_{max}$  value, which appears as dashed line for reference.

The estimate of  $P(t)$  was obtained applying the STA described in (9) which can be obtained using the residual ozone flowing out from the reactor, which is a measurable online variable. This estimation was done considering the presence of output noise produced by the gas ozone concentration. This method was implemented with the parameters  $\gamma_1 = 3.65$ ,  $\gamma_2 = 11.35$ . This experimental auxiliary estimate  $\hat{P}(t)$  reaches the value of  $P(t)$  after 35.0 seconds (Figure 14).

Based on finite-time recovery of  $P(t)$ , the estimate of the contaminant concentration was attained after 7.0 seconds. However, the linear nature of the parametric estimation method introduces asymptotic convergence of the contaminant estimation. Figure 15 demonstrates the comparison of the actual contaminant variation and its estimate. Notice that both trajectories decrease at the same rate.

The parametric identification method proposed in (7) estimates the reaction rate constant  $k_1$  after 100 seconds. This estimate asymptotically recovered the true value of the reaction rate constant of ozone with the proposed contaminant (Figure 16).

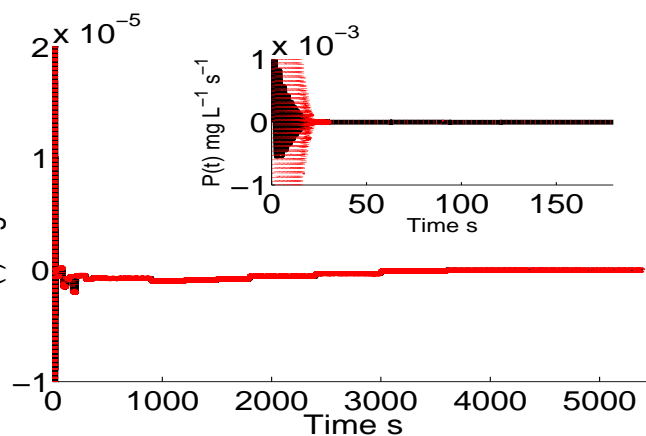


Fig. 14. The comparison of measured contaminant decomposition rate (solid line, marker \*) and the estimated by the method proposed in this study (dotted line) based on the online reconstruction by the STA implemented as differentiator. The closer view demonstrates the first 170 seconds of simulation to highlight the faster estimation of  $P(t)$ .

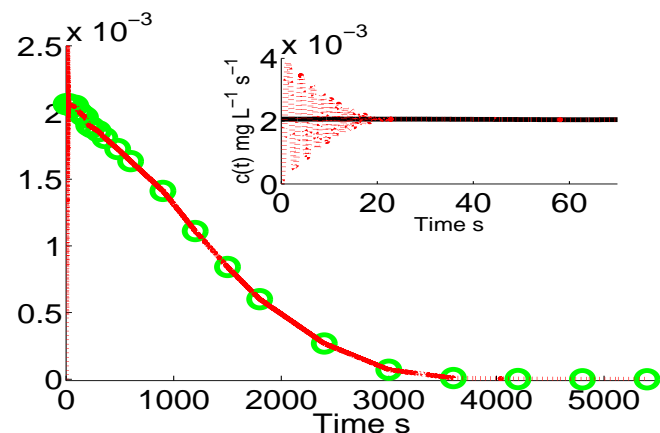


Fig. 15. The comparison of the phenol concentration  $c_1(t)$  (solid line, marker \*) and the estimated by the method  $\hat{c}_1(t)$  proposed in this study (dotted line) for the ozonation of the real contaminated water.

## 8. CONCLUSIONS

This study presents a new continuous-time method intended to develop the simultaneous state and parameter estimation of ozonation, based on the proportional-integral version of the Least Mean Square method. The proposed method estimates the reaction rate constants and concentrations of the contaminants reacting with ozone in the liquid phase of a chemical reactor. The proposed method, applied for the state estimation, implements the STA as a robust differentiator to obtain the contaminant decomposition rates online. This information is used in the parameter estimation procedure. The method has been tested on two specific cases in the presence of one and two contaminants. Also, this method has been evaluated using experimental laboratory data for one contaminant (phenol), assuming that only the reactors' ozone gas concentration is available online. The suggested method has demonstrated an extremely high quality of the resulting state and parameter estimation.

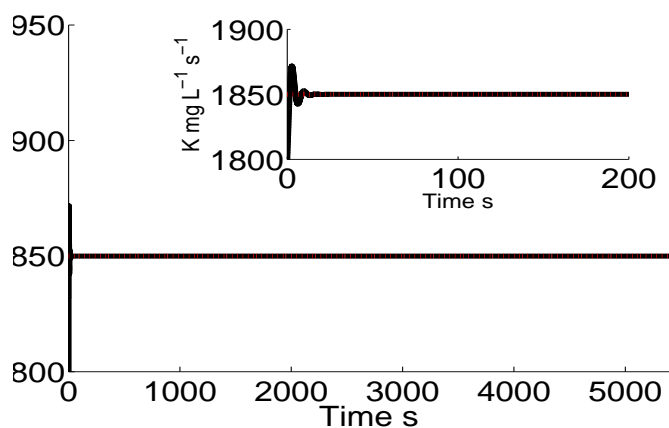


Fig. 16. The comparison of reported contaminant reaction rate constant  $k_1(t)$  (solid line) and the parameter estimated by the method  $\hat{k}_1(t)$  proposed in this study (dotted line) in the case of ozonation of phenol. The reference value was obtained from the work presented by [19]-Chapter5.

#### ACKNOWLEDGEMENT

The authors thank the financial support provided by the **Newton Fund (Project 278228)** through the **Institutional Links Call** associated to the **Fondo de Cooperación Internacional de Ciencia y Tecnología (FONCYCYT)**.

#### CONFLICT OF INTEREST

Conflict of interest - none declared

#### REFERENCES

- [1] P. R. Gogate and A. B. Pandit, "A review of imperative technologies for wastewater treatment i: oxidation technologies at ambient conditions," *Advances in Environmental Research*, vol. 8, no. 3-4, pp. 501–551, 2004.
- [2] C. Von Sonntag and U. Von Gunten, *Chemistry of ozone in water and wastewater treatment*. IWA publishing, 2012.
- [3] J. E. Schollée, M. Bourgin, U. von Gunten, C. S. Mc Ardell, and J. Hollender, "Non-target screening to trace ozonation transformation products in a wastewater treatment train including different post-treatments," *Water research*, 2018.
- [4] D. Gerrity, F. L. Rosario-Ortiz, and E. C. Wert, "Application of ozone in water and wastewater treatment," *Advanced Oxidation Processes for Water Treatment: Fundamentals and Applications*, p. 123, 2017.
- [5] K. Ikehata and Y. Li, "Ozone-based processes," in *Advanced Oxidation Processes for Waste Water Treatment*, pp. 115–134, Elsevier, 2018.
- [6] A. Tawk, M. Deborde, J. Labanowski, S. Thibaudeau, and H. Gallard, "Transformation of the b-triketone pesticides tembotrione and sulcotrione by reactions with ozone: Kinetic study, transformation products, toxicity and biodegradability," *Ozone: Science & Engineering*, vol. 39, no. 1, pp. 3–13, 2017.
- [7] N. Maya, J. Evans, D. Nasuhoglu, S. Isazadeh, V. Yargeau, and C. D. Metcalfe, "Evaluation of wastewater treatment by ozonation for reducing the toxicity of contaminants of emerging concern to rainbow trout (oncorhynchus mykiss)," *Environmental toxicology and chemistry*, vol. 37, no. 1, pp. 274–284, 2018.
- [8] F. Lüddecke, S. Heß, C. Gallert, J. Winter, H. Güde, and H. Löffler, "Removal of total and antibiotic resistant bacteria in advanced wastewater treatment by ozonation in combination with different filtering techniques," *Water research*, vol. 69, pp. 243–251, 2015.
- [9] M. S. Lucas, N. M. Reis, and G. L. Puma, "Intensification of ozonation processes in a novel, compact, multi-orifice oscillatory baffled column," *Chemical Engineering Journal*, vol. 296, pp. 335–339, 2016.
- [10] M. Bourgin, E. Borowska, J. Helbing, J. Hollender, H.-P. Kaiser, C. Kienle, C. S. Mc Ardell, E. Simon, and U. Von Gunten, "Effect of operational and water quality parameters on conventional ozonation and the advanced oxidation process o3/h2o2: Kinetics of micropollutant abatement, transformation product and bromate formation in a surface water," *Water research*, vol. 122, pp. 234–245, 2017.
- [11] M. Lee, L. C. Blum, E. Schmid, K. Fenner, and U. Von Gunten, "A computer-based prediction platform for the reaction of ozone with organic compounds in aqueous solution: kinetics and mechanisms," *Environmental Science: Processes & Impacts*, vol. 19, no. 3, pp. 465–476, 2017.
- [12] Y. Lee and U. Von Gunten, "Advances in predicting organic contaminant abatement during ozonation of municipal wastewater effluent: reaction kinetics, transformation products, and changes of biological effects," *Environmental Science: Water Research & Technology*, vol. 2, no. 3, pp. 421–442, 2016.
- [13] S. Yousefian, G. Bourque, and R. F. Monaghan, "Uncertainty quantification of nox emission due to operating conditions and chemical kinetic parameters in a premixed burner," *Journal of Engineering for Gas Turbines and Power*, vol. 140, no. 12, p. 121005, 2018.
- [14] R. L. Sternberg, *Nonlinear Partial Differential Equations in Engineering and Applied Science: Volume 54*. Routledge, 2017.
- [15] A. Tulsyan, B. Huang, R. B. Gopaluni, and J. F. Forbes, "On simultaneous on-line state and parameter estimation in non-linear state-space models," *Journal of Process Control*, vol. 23, no. 4, pp. 516–526, 2013.
- [16] S. B. Chitralkha, J. Prakash, H. Raghavan, R. Gopaluni, and S. L. Shah, "A comparison of simultaneous state and parameter estimation schemes for a continuous fermentor reactor," *Journal of Process Control*, vol. 20, no. 8, pp. 934–943, 2010.
- [17] X. Hulhoven, A. V. Wouwer, and P. Bogaerts, "State observer scheme for joint kinetic parameter and state estimation," *Chemical engineering science*, vol. 63, no. 19, pp. 4810–4819, 2008.
- [18] M. Soroush, "State and parameter estimations and their applications in process control," *Computers & Chemical Engineering*, vol. 23, no. 2, pp. 229–245, 1998.
- [19] T. Poznyak, I. Chairez, and A. Poznyak, *Ozonation and Biodegradation in Environmental Engineering: Dynamic Neural Network Approach*. Elsevier, 2019.
- [20] A. Biń, "Ozone dissolution in aqueous systems treatment of the experimental data," *Experimental Thermal and Fluid Science*, vol. 28, no. 5, pp. 395–405, 2004.
- [21] A. K. Biń, "Ozone transfer from gas into water and contact equipment design," *Encyclopedia of Life Support Systems (EOLSS)-UNESCO*, vol. 6, 2008.
- [22] G. S. Bhosale, P. D. Vaidya, J. B. Joshi, and R. N. Patil, "Kinetics of ozonation of phenol and substituted phenols," *Industrial & Engineering Chemistry Research*, vol. 58, no. 18, pp. 7461–7466, 2019.
- [23] C. Gottschalk, J. A. Libra, and A. Saupe, *Ozonation of water and waste water: A practical guide to understanding ozone and its applications*. John Wiley & Sons, 2009.
- [24] T. Poznyak, I. Chairez, and A. Poznyak, *Ozonation and biodegradation in environmental engineering: Dynamic neural network approach*. Elsevier, 2018.
- [25] K. L. Rakness, *Ozone in drinking water treatment: process design, operation, and optimization*. American Water Works Association, 2011.
- [26] T. I. Poznyak, A. Manzo, and J. L. Mayorga, "Elimination of chlorinated unsaturated hydrocarbons from water by ozonation: Simulation and experimental data comparison," *Revista de la Sociedad Química de México*, vol. 47, no. 1, pp. 58–65, 2003.
- [27] A. Levant, "Robust exact differentiation via sliding mode technique," *Automatica*, vol. 34, no. 3, pp. 379–384, 1998.
- [28] X.-G. Yan, S. K. Spurgeon, and C. Edwards, *Variable Structure Control of Complex Systems*. Springer, 2017.
- [29] I. Castillo, L. Fridman, and J. Moreno, "Super-twisting algorithm in presence of time and state dependent perturbations," *International Journal of Control*, vol. 91, no. 11, pp. 2535–2548, 2018.
- [30] R. Seeber, M. Horn, and L. Fridman, "A novel method to estimate the reaching time of the super-twisting algorithm," *IEEE Transactions on Automatic Control*, 2018.
- [31] J. Escobar and A. Poznyak, "Parameter estimation in continuous-time stochastic systems with correlated noises using the kalman filter and least squares method," *IFAC-PapersOnLine*, vol. 51, no. 13, pp. 309–313, 2018.

## 9. APPENDIX

The parameter identification algorithm proposed in (7) can be presented as follows

$$\begin{aligned} \frac{d}{dt} \hat{k}_i(t) &= -\alpha_i(t) J_i(t) - \delta_{P_i} \Delta_k(t) - \delta_{I_i} \hat{l}_i(t) \\ \frac{d}{dt} \hat{l}_i(t) &= \Delta_{k_i}(t) \end{aligned}$$

The dynamics of  $\Delta_k$  satisfies

$$\begin{aligned} \frac{d}{dt} \Delta_{k_i}(t) &= -\alpha_i(t) J_i(t) - \delta_{P_i} \Delta_k(t) - \delta_{I_i} \hat{l}_i(t) \\ \frac{d}{dt} \hat{l}_i(t) &= \Delta_{k_i}(t) \end{aligned}$$

with

$$\frac{d}{dt} J_i(t) = -a(t) J_i(t) + a(t) g_i(t), \quad a(t) = (t + \varepsilon)^{-1}$$

The function  $g_i(t)$  is governed by

$$g_i(t) = \Delta_P(t) \left[ 1 - \Delta_{k_i}(t) \varphi(t) - \hat{k}_i \varphi(t) \right]$$

with

$$\Delta_P(t) = - \sum_{i=1}^N \left( \hat{k}_i \hat{c}_i(t) - k_i c_i(t) \right) Q(t).$$

The term  $\Delta_P$  can be transformed into

$$\begin{aligned} \Delta_P(t) &= - \sum_{i=1}^N \left( \Delta_{k_i}(t) \hat{c}_i(t) + \hat{k}_i \Delta c_i(t) + \Delta \hat{k}_i \hat{c}_i(t) \right) Q(t) \\ \Delta c_i(t) &= \hat{c}_i(t) - c_i(t), \quad \Delta \hat{k}_i = \hat{k}_i - k_i \end{aligned}$$

The term  $\Delta c_i(t)$  satisfies the following dynamics

$$\frac{d}{dt} \Delta c_i(t) = - \left( \Delta_{k_i}(t) \hat{c}_i(t) - k_i \Delta c_i(t) \right) \frac{Q(t)}{V_{liq}}$$

Notice that the dynamics of  $z$  is governed by

$$\frac{d}{dt} z(t) = \Lambda^0 z(t) + (\Lambda(t) - \Lambda^0) z(t) + \Gamma(t) \quad (15)$$

To prove that the origin is a practically stable equilibrium point of (11), lets propose the Lyapunov function candidate

$$V(z) = z^\top P z \quad (16)$$

The full-time derivative of  $V(z)$  (evaluated over the trajectories of  $z$ ) satisfies

$$\begin{aligned} \frac{d}{dt} V(z(t)) &= 2z^\top(t) P [\Lambda^0 z(t)] \\ 2z^\top(t) P [(\Lambda(t) - \Lambda^0) z(t) + \Gamma(t)] &= \\ z^\top(t) [P\Lambda^0 + \Lambda^{0\top} P] z(t) + & \\ 2z^\top(t) P (\Lambda(t) - \Lambda^0) z(t) + 2z^\top(t) P \Gamma(t) & \end{aligned} \quad (17)$$

The direct application of the Young's matrix inequality:  $X^\top Y + Y^\top X \leq X^\top \Pi X + Y^\top \Pi^{-1} Y$ , valid for any  $X$ ,

$Y \in \mathbb{R}^{\kappa \times \kappa}$  and any  $0 < \Pi$ ,  $\Pi = \Pi^\top$ ,  $\Pi \in \mathbb{R}^{\kappa \times \kappa}$  and considering that  $\Pi_0 = \pi I$ ,  $\|\Lambda(t) - \Lambda^0\|^2 \leq q$ , yields

$$\begin{aligned} 2z^\top(t) P (\Lambda(t) - \Lambda^0) z(t) &\leq \\ z^\top(t) P \Pi_0^{-1} P z(t) + & \\ z^\top(t) (\Lambda(t) - \Lambda^0)^\top \Pi_0 (\Lambda(t) - \Lambda^0) z(t) &\leq \\ \pi^{-1} z^\top(t) P^2 z(t) + \pi z^\top(t) \|\Lambda(t) - \Lambda^0\|^2 z(t) &\leq \\ \pi^{-1} z^\top(t) P^2 z(t) + \pi q z^\top(t) z(t) = & \\ z^\top(t) [\pi^{-1} P^2 + \pi q I_{4N \times 4N}] z(t) & \end{aligned} \quad (18)$$

If it is considered that  $\Pi = P$ , then

$$2z^\top(t) P \Gamma(t) \leq \|\Gamma(t)\|_\Pi^2 + z^\top(t) P \Pi^{-1} P z(t) \quad (19)$$

The substitution of (18) and (19) in (17) implies

$$\begin{aligned} \frac{d}{dt} V(z(t)) &\leq \|\Gamma(t)\|_\Pi^2 + \\ z^\top(t) [P\Lambda^0 + \Lambda^{0\top} P + P + \pi^{-1} P^2 + \pi q I_{4N \times 4N}] z(t) & \end{aligned} \quad (20)$$

Introduce a matrix  $\dot{P}$ , satisfying  $\pi^{-1} P^2 < \dot{P}$ . By the Schur complement ([19]) this inequality holds if and only if

$$\begin{bmatrix} \dot{P} & P \\ P & \pi I_{4N \times 4N} \end{bmatrix} > 0 \quad (21)$$

The differential equation (20) is valid if

$$\begin{aligned} \frac{d}{dt} V(z(t)) &\leq \|\Gamma(t)\|_\Pi^2 + \\ z^\top(t) [P\Lambda^0 + \Lambda^{0\top} P + P + \dot{P} + \pi q I_{4N \times 4N}] z(t) & \end{aligned} \quad (22)$$

The differential inclusion (22) is equivalent to

$$\begin{aligned} \frac{d}{dt} V(z(t)) &\leq z^\top(t) [P\Lambda_\alpha^0 + \Lambda_\alpha^{0\top} P + \dot{P} + \pi q I_{4N \times 4N}] z(t) \\ -\alpha z^\top(t) P z(t) + \|\Gamma(t)\|_\Pi^2 & \end{aligned} \quad (23)$$

The application of the upper-bound for  $\Gamma(\beta)$  on (23) leads to

$$\frac{d}{dt} V(z(t)) \leq -\alpha V(z(t)) + \beta \quad (24)$$

The application of the comparison principle and the solution for the equality in (24) justifies that  $\limsup_{t \rightarrow \infty} V(t, z(t)) \leq \frac{\beta}{\alpha}$  which implies the inequality

$$\limsup_{t \rightarrow \infty} \|z(t)\| \leq \sqrt{\frac{\beta}{\alpha \cdot \lambda_{\min} \{P^m\}}}$$